Clear processing of infrared images of dust during underground excavation

2024 9th International Conference on Image, Vision and Computing (ICIVC) | 979-8-3503-8599-1/24/$31.00 ©2024 IEEE | DOI: 10.1109/ICIVC61627.2024.10837324

Wentao Liu
School of Computer and Artificial Intelligence
Beijing Technology and Business University
2926935343@qq.com
China Beijing

Tao Xie
School of Computer and Artificial Intelligence
Beijing Technology and Business University
xietao@btbu.edu.cn
China Beijing

Zheng Tong
School of Computer and Artificial Intelligence
Beijing Technology and Business University
20211206@btbu.edu.cn
China Beijing

***Abstract*—In the underground drilling environment, visible light has poor ability to capture information in dust under dark illumination, so infrared cameras are used to collect data. Although infrared images can greatly improve the capture of detailed information compared with visible light images, the image quality is still affected by imaging blur caused by high temperature of equipment and dust in drilling. Therefore, it is necessary to clear the infrared image processing. Some infrared image sharpening algorithms based on prior dark channels will have some problems such as too dark image, color deviation, distortion and incomplete fog removal when processing infrared images of underground dust environment, and there will be some noise that does not exist originally. Combining these problems, an improved dark channel prior fog removal algorithm is proposed, which is divided into three parts. First, the atmospheric light value is optimized by improving the color image classification, and then the atmospheric scattering model is optimized by adding boundary constraints to the transmittance. The resulting image transmittance is refined by double-weighted filtering. At last, the image is enhanced to improve the brightness of the image, and the image after sharpening is evaluated.**

Keywords—underground dense fog, infrared image, dark channel prior, image enhancement, transmittance

I. INTRODUCTION

The image clarity algorithm has a wide range of applications in fields such as transportation, security, medical, and military. Nowadays, with the increasing application of electronic device visualization, the clarity of underground images has become a hot topic. Underground excavation operation refers to the activity of workers operating tunneling machines to excavate and extract resources such as coal mines in the dark underground environment. Due to factors such as weak underground light sources, the imaging effect of visible light images is poor.

During underground excavation operations, infrared equipment imaging is usually used to solve this problem, but the dust generated during the excavation process has a high temperature, which affects the infrared imaging and reduces its clarity. The scattering effect of particles in the atmosphere of the scene can cause a decrease in the imaging quality of infrared acquisition equipment, affecting the discrimination of scene information by workers in dust, and creating significant safety hazards. This shows the importance of image clarity.

Classic image clarity mainly includes: 1) algorithms based on image enhancement; 2) Image restoration algorithm based on physical models; 3) Algorithm based on deep learning[10].

The image restoration algorithm based on physical models mainly analyzes the physical process of imaging and establishes a physical imaging model [7], which can reflect the relationship between clear images and blurred images. Based on this, He et al [16]. proposed a dark channel prior theory, which estimates the transmittance and dark channel method to calculate the atmospheric light value from a clear image [8]. However, this method estimates the atmospheric light value as a constant, which can weaken the image clarity effect [15] and cause halo phenomena in the image.

The image clarity algorithms based on deep learning have also rapidly developed. Convolutional neural networks are most commonly used in the field of image processing [9]. Cai et al. proposed a DehazeNet network [11][12], while Chen et al. proposed an end-to-end deblurring algorithm [14]. This method effectively solves the problem of image artifacts after clarity, but it is not suitable for processing infrared images of underground dust in this paper.

The principle of image enhancement algorithm is to highlight the visual effect of the image through contrast enhancement, thereby achieving clarity[1]. However, this method does not consider the root cause of image blur, which can lead to other factors affecting the image quality after processing by some enhancement algorithms[13]. The commonly used algorithms for induction include histogram equalization [2][3], Rentinex enhancement algorithm [4][6], wavelet transform algorithm [5], etc. The conventional image enhancement algorithm is too simple, and when processing the underground infrared images in this article, it will cause problems such as distortion, patches, and excessive contrast.

In response to the characteristics of dark and noisy infrared image scenes of underground dust, a processing method based on image restoration is selected, and algorithm and model

improvements are made to address the noise and halo problems existing in classical dark channel priors. The clarity effect is improved by optimizing atmospheric light value, transmittance, and filtering the transmittance map. After experimental verification, this method has shown good performance in deblurring infrared images of underground dust.

II. Related work

A. Prior principle of dark channel

The dark channel prior is a deblurring algorithm proposed by He et al., which is based on physical model restoration. The atmospheric model used is described as follows:

$$I(x) = J(x) + A[1 - t(x)] \tag{1}$$

$I(x)$ represents the dust image, and $J(x)$ represents the image after deblurring; A is the atmospheric light value; X is the coordinate pixel; The transmittance graph represented by $t(x)$.

The prior theory of dark channel is to define the dark channel of an image, which means that except for the sky region, the intensity of J tends to zero when it is low. The formula is as follows:

$$J^{dark}(x) = \min_{c \in (r,g,b)} (\min_{y \in \Omega(x)} (J^c(y)) \tag{2}$$

Among them, $J(y)$ is a color component in a color haze free image, and $\Omega(x)$ is the neighborhood centered on pixel x in the image. The atmospheric light value A of this algorithm is obtained from the brightest pixel point in the dark channel. By combining equations (1) and (2), the following transformation can be obtained:

$$\min_{y \in \Omega(x)} (I^C(y)) = \tilde{t}(x) \min_{y \in \Omega(x)} (J(y)) + (1 - \tilde{t}(x)) A^c \tag{3}$$

In the prior dark channel algorithm, the dark channel J of the Ambiguous atmospheric light radiation J tends towards zero, resulting in dark $J(x)=0$, and Ac is always positive, which leads to:

$$\min_c (\min_{y \in \Omega(x)} (\frac{J^c(y)}{A^c})) = 0 \tag{4}$$

After substituting (2), (3), and (4) into (1), the estimated transmittance can be obtained as follows:

$$\bar{t}(x) = 1 - \min_c (\min_{y \in \Omega(x)} (\frac{J^c(y)}{A^c})) \tag{5}$$

Based on the obtained transmittance, further refinement can be taken to obtain the restored image according to formula (1).

III. Model improvement based on dark channel prior

The infrared images of underground dust are different from general infrared images. The shooting scene of the infrared images of excavation is a real underground coal mine operation scene, and there is no sky area with poor prior dark channel algorithm processing. In addition, the brightness of the light in the scene is poor, and the fog in the scene, as well as the dust and smoke with temperature generated by the excavation drill bit during operation, can all affect the infrared imaging equipment. In addition, due to the influence of atmospheric light estimation bias, the gray and white areas or high contrast points in infrared images undergo color shift [15]. When there are few light sources and large dust in the scene, using traditional dark channel prior algorithms to process images may result in incomplete deblurring and overall darkening of the image. This article proposes an optimization algorithm based on dark channel priors to address these issues. The specific steps for improving the algorithm are as follows:

1) Calculate the dark channel for foggy images, use the prior method of dark channel to calculate the atmospheric light value, and optimize the acquisition of atmospheric light.

2) According to the transmittance calculation method of the dark channel prior algorithm, boundary constraints are added to J (x) based on the information of the image to obtain the transmittance of the constraint conditions.

3) Applying a bilateral weighted filtering method for transmittance refinement, combining atmospheric light values and optimized transmittance into the scattering model to restore the image.

4) Based on the image obtained after deblurring, the Laplace operator is used to sharpen the image, enhancing its contrast and improving its clarity.

A. Optimization of atmospheric light value

The classic dark channel prior algorithm is affected by the light source points when calculating atmospheric light, which reduces the deblurring efficiency. Therefore, an improvement was made by taking the top 1% pixels with the highest brightness in the dark channel, and using the average value of the pixels corresponding to the dust image as the atmospheric light value, and optimizing the parameters. Namely:

$$Ac = \frac{1}{|P_D|} \sum_{x \in P_D} I_C'(x), \forall c \in \{r,g,b\} \tag{6}$$

Among them, P_D represents the top 1% pixels.

Classify foggy images based on whether they have color deviation, and the chromaticity diffusion of an image is an important feature for distinguishing whether an image has color deviation [18]. Define chromaticity diffusion as:

$$MOS = \frac{1}{MN} \sum_x \sum_y \delta(x,y) \tag{7}$$

$$\delta = \min\{[\mu - h(x,y)]^2, [1 - |\mu - h(x,y)|]^2\} \tag{8}$$

Among them, μ It is the mean chromaticity, and $h(x, y)$ is the chromaticity of pixels with coordinates $h(x, y)$ in an image of size $M \times N$. Using the method of minimizing classification error to distinguish between biased and unbiased images, the

critical *MOS* is used as the threshold. If it is less than 0.01, it is determined that there is color deviation [19].

When processing images with color bias, define $\eta = \frac{\mu_c}{\mu_{\max}}$, μ_c is the mean of channel c. $\mu_{\max} = \max_{i\in(r,g,b)}$, I' formula is as follows:

$$I_c'(x) = \min[I_c^{\eta}(x), \max_{i\in(r,g,b)} I_c(x)] \tag{9}$$

Optimize atmospheric lighting based on color deviation:

$$\alpha_c = (\frac{A_{\max}}{A_c})^{\sqrt{k_c}} \tag{10}$$

Wherein, $A_{\max} = \max_{c\in(r,g,b)}$, $K_c = 2\sqrt{v}$,V is the *MOS* value, and the final optimized atmospheric light value is obtained:

$$A_c = \frac{A_c}{\alpha_c} \tag{11}$$

B. Calculate the transmittance

According to the classical dark channel prior formula, the expression for transmittance can be derived:

$$\frac{1}{t(x)} = \frac{\| J(x) - A \|}{\| I(x) - A \|} \tag{12}$$

Based on the two constant vectors C_0 and C_1 of the given image, impose conditional constraints on $J(x)$ for each pixel point x:

$$C_0 \le J(x) \le C_1, \forall x \in \Omega \tag{13}$$

$$t_b(x) = \min\{\max_{c\in\{r,g,b\}}(\frac{A^c - I^c(x)}{A^c - \mathrm{C}_0^c}, \frac{A^c - I^c(x)}{A^c - \mathrm{C}_1^c}), 1\} \tag{14}$$

Among them, I_c, A_c, C_0^c , and C_1^c are the color channels of I, A, C_0, and C_1, respectively.

C. Bilateral weighted filtering for refining transmittance

The classic guided filtering may have halo artifacts when processing transmittance maps, as the linear model and regularization parameters are uniformly applied to the entire image. Therefore, the objective function is improved by introducing weights $w_{i,k}$ after the least squares formula. The new objective function is as follows:

$$E(a_k, b_k) = \sum_{i\in\Omega k}[w_{i,k}(a_k I_i + b_k - p_i)]^2 + \frac{e}{\Omega} a_k^2] \tag{15}$$

Where e/Ω is a constant parameter, w is the calculated weight, p is the input, and the calculation formulas for ak and bk are as follows:

$$a_k = \frac{\sum_{i\in\Omega k} w_{i,k} I_i P_i - \sum_{i\in\Omega k} w_{i,k} I_i}{\sum_{i\in\Omega k} w_{i,k} {I_i}^2 - (\sum_{i\in\Omega k} w_{i,k} I_i)^2 + e} \tag{16}$$

$$b_k = \sum_{i\in\Omega k} w_{i,k} p_i - a_k \sum_{i\in\Omega k} w_{i,k} I_i \tag{17}$$

Similarly, a pixel will be included in multiple windows, and the output point needs to calculate the weighted average of all linear function values containing that point. The formula for calculating the weighted average is:

$$qi = \sum_{i\in\Omega i} w_{i,k} a_i I_i + \sum_{i\in\Omega k} w_{i,k} b_i \tag{18}$$

Choose a bilateral kernel function to calculate weights, i.e:

$$w_{i,k} = \frac{1}{k} D_{i,j} R_{i,j} \tag{19}$$

$$D_{i,j} = \exp(-\frac{\|j-i\|^2}{2\sigma_r^2}) \tag{20}$$

$$D_{i,j} = \exp(-\frac{\|j-i\|^2}{2\sigma_r^2}) \tag{21}$$

Where K is the dimensional normalization constant, σ_D is the spatial variance; σ_R is the range variance. When processing image edge regions, there is a significant change in pixel values, and the pixel range domain weights maintain edge information[23].

The implementation of bilateral weighted guided image filtering first inputs image p, guided image I, window radius, regularization coefficient, and variance. After calculation, the final output image q is obtained. The specific implementation is as follows:

1） $w_I = f_{domain}(I) \cdot f_{rang}(I)$

2） $wavg_I = f_{wavg}(I), wavg_p = f_{wavg}(p), wavg_{II} = f_{wavg}(I \cdot I)$
$wavg_{Ip} = f_{wavg} = (I \cdot p)$

3） $a = \frac{wavg_{IP} - wavg_p \cdot wavg_I}{wavg_{II} - (wavg)^2 + e}, b = wavg_P - a \cdot wavg_I$

4） $\mathrm{wavg}_a = f_{wavg} wavg_b = f_{wavg}(b)$

5） $q = wavg_a I + wavg(b)$

Among them, f_{domian} and range are calculated by equations (20) and (21), and f_{wavg} represents the calculation of weighted average. P is the input image, I is the guide image, the window radius is r, and e is the regularization coefficient.

D. Image sharpening processing using Laplace operator

Due to the fact that in most cases, noise is also enhanced after image sharpening, Gaussian filtering is first used to smooth the image, and then Laplace operator is used to sharpen the image. The Laplace operator for two-dimensional image *f (x, y)* is defined as:

$$\nabla^2 f(x,y) = f(x+1,y) + f(x,y+1) + f(x,y-1) - 4f(x,y) \tag{22}$$

Among them, $g(x, y)$ represents the sharpened image, and $f(x, y)$ represents the pre sharpened image.

Next, by constructing a Laplace template and expanding from four neighborhoods to eight neighborhoods, the obtained values are replaced with the original pixel values. Finally, the image is obtained using the sharpening formula, as follows:

$$g(x,y) = f(x,y) - [\nabla^2 f(x,y)] \tag{23}$$

IV. Experimental results

This article uses Matlab2016a as the experimental operating platform and operates on a Windows 10 system with 16GB of memory. Firstly, the transmittance map after obtaining the constraint conditions is processed using several different filtering methods to present the optimization effect of the bilateral weighted filtering selected in this article more clearly. This results in an objective evaluation of the filtering process.As shown in Figure 1, this article tested five different transmittance processing methods, as shown in Figure1. Among them, (a) is the original transmittance map obtained in this article, (b) is the image processed by gradient threshold filtering algorithm, (c) is a bilateral weighted filtering algorithm based on guided filtering selected in this article, (d) is an improved edge perception weight guided filtering algorithm proposed by Lu et al., (e) and (f) Corresponding to the soft cutout and classical guided filtering algorithms for optimizing transmittance maps in the dark channel prior algorithm proposed by He et al., respectively.

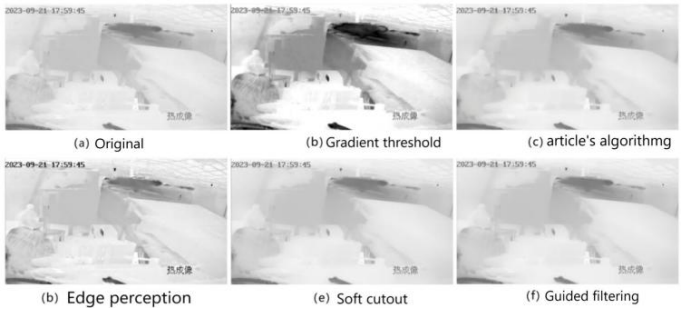

Figure. 1 .Comparison of Refinement Processing for Transmission Chart.

Due to the unclear visual effect of the filtered transmittance map, this article compares the effectiveness of transmittance optimization by calculating the peak signal-to-noise ratio and structural similarity between the original transmittance map and the processed image. The specific data is shown in Table 1:

TABLE I. Peak signal-to-noise ratio and structural similarity corresponding to different methods of optimizing transmittance maps

evaluation	*PSNR*	*SSIM*
Article's algorithm	30.85	0.4458
Gradient threshold	12.17	0.2456
Guided filtering	31.77	0.3611
Soft Cutout	29.56	0.3934
Edge Perception	26.04	0.5171

After comparison, the *PSNR* of the transmittance map processed by bilateral weighted filtering in this article is higher than that of soft thresholding, gradient threshold filtering, and edge perception filtering, and the SSIM value is higher than that of guided filtering, soft thresholding, and gradient threshold filtering. The application of this filtering algorithm can be well applied to infrared imaging scenes of underground dust. In order to demonstrate the advantages of the clarity algorithm in processing infrared images of underground dust in this article, a comparison was made between the clarity algorithm that is more suitable for the scene and has better clarity processing effects, and the classic prior dark channel algorithm.

(a) represents the image before processing, (b) and (c) represent the soft cutout of He and the deblurring image processed by the guided filtering algorithm [21], respectively. (d) is a novel dark channel prior guided variational framework proposed by Hou Guojia and others for underwater image restoration algorithms [22].(e) is Chuanzi He's haze density perception adaptive perception single image deblurring algorithm, and (f) is the clarity algorithm of this paper. As shown in Figure 2:

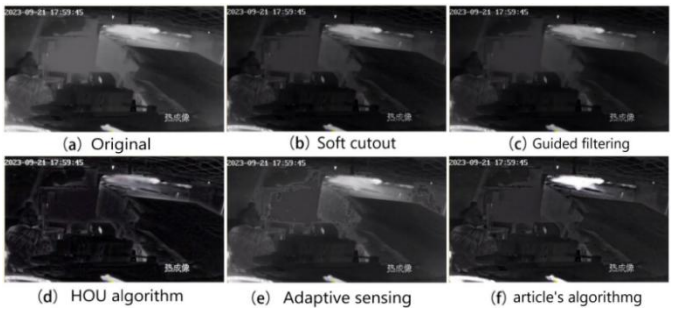

Figure. 2 .Comparison of Different Deblurring Algorithms.

Through comparison, it can be seen that He's soft cutout and guided filtering algorithms are not suitable for the infrared images of this scene, and the details of the dark areas after processing are not obvious, resulting in poor clarity for dust blurred areas. The images processed by Hou et al.'s guided variational framework show obvious details, but the overall contrast is too high and the dust treatment effect is not good. He's haze adaptive algorithm has many patches, so it is not suitable for this scene.

The algorithm in this article can effectively handle the dust generated during excavation by the tunneling machine, with a clear effect and good retention of details in dark areas. Calculate the peak signal-to-noise ratio and structural similarity ratio between the deblurring images obtained by different algorithms and the original image, shown in Table 2:

TABLE II. PEAK SIGNAL-TO-NOISE RATIO AND STRUCTURAL SIMILARITY CORRESPONDING TO DIFFERENT DEBLURRING ALGORITHMS

evaluation	*PSNR*	*SSIM*
Article's algorithm	18.21	0.8299
Soft Cutout	17.38	0.6021
Guided filtering	17.61	0.6465
Adaptive sensing	23.03	0.7501
Hou algorithm	15.76	0.5485

By comparison, it can be seen that the PSNR of the infrared image after the algorithm in this article is higher than He's guidance filtering algorithm, soft cutout algorithm, and Hou's algorithm, and SSIM is higher than other algorithms.The clarity algorithm in this article is more suitable for infrared images of underground sand and dust scenes.

To further improve the clarity of the image, this article adopts image sharpening processing based on Laplace operator, which improves the contrast of the image and solves the problem of too dark image details. After sharpening, the contrast of the image has been improved, not only handling dust and smoke in the scene, but also better reflecting the detailed information in the image. As shown in Figure 3:

Fig. 3. Example of a figure caption.

V. SUMMARIZE

A novel method for clarifying infrared images of underground dust is proposed in the article, which improves the accuracy of atmospheric light value estimation through color deviation classification, adds constraints to calculate the normal transmittance wave, and embeds bilateral weighting into the guiding filter to avoid halo artifacts and remove noise.

Through qualitative experiments in image processing, it has been proven that bilateral weighted guided filtering can effectively process the transmittance map of infrared images of underground dust, thereby improving the clarity of the dark channel prior algorithm. Finally, combining Laplace operator for sharpening, subjectively improves the visual effect of the image after sharpening. Finally, after calculation, the PSNR and SSIM of the images processed by the algorithm used in this article reached 18.21 and 0.8299, respectively.

REFERENCES

[1] S. Salazar Colores, I. Cruz Aceves, J.Ramos Arreguin and M, "Single image dehazing using a multilayer perceptron," *Journal of Electronic Imaging. vol*. 27, no. 4, Apr.2018.

[2] J. Kim, L. Kim, and S. Hwagn, "An advanced contrast enhancement using partially overlapped sub-block histogram equalization," IEEE Trans Circuits Syst Video Techno, vol. 11, no. 4, pp:475–484, Apr. 2001.

[3] S. Liu, C. Sun, H. Lou, Y. Long and T. Xu. "Research on image dehazing based on histogram equalization and Retinex, " *Information and computers.* vol. 35, no.15, pp:13-24, Apr.2023.

[4] M. Zheng. "Image dehazing and denoising algorithm based on Retinex theory," *Intelligent Computer and Applications*, no. 2, pp: 93-96, Apr.2020,10.

[5] H. He,TuerhongjiangAbudukilimu and X. He. "Traffic Image Defogging Method Based on Wavelet Transform,". *Electronic Design Engineering*, vol.28, no.28 , pp: 56-59, Apr.2020.

[6] RUSSO F. "An image enhancement technique combining sharpening and noise reduction,". *IEEE Transactions on Instrumentation and Measurement*, vol.51, no.4, pp:824–828, Apr.2002.

[7] J. Gao, Q. Chu, X. Zhang and Z Fan. "Image dehazing method combining light field depth estimation and atmospheric scattering model,". *Acta Photonica Sinica*, vol. 49, no.7, pp:23–34, Apr:2020.

[8] K. He, J. Sun and X. Tang. "Single image haze removal using dark channel priority," *IEEE Transactions on Pattern Analysis and Machine Intelligence*, vol.33, no.12, pp:2341–2353, Apr:2011.

[9] A. Yang, J. Liu, J. Xing, X. Li and Y. He."A single image dehazing network based on the fusion of content and style features," *Journal of Automation*, vol.07, no.10, pp: 1–11, Apr:2020.

[10] D.Wang, T.Zang ."Review and analysis of image dehazing algorithms,". *Journal of Graphics*. vol.6, no.12, pp: 1–11, Apr:2020.

[11] B. Cai, X.Xu, K. Jia and C.Qing, D Tao. "Dehazenet:An end to end system for single image haze removal," *IEEE Transactions on Image Processing*, vol.25, no.11, pp:5187–5198. Apr.2016.

[12] K. Yuan, J. Wei and W. Lu. "Single Image Dehazing via NIN DehazeNet," *IEEE Access*, no.7, pp:181348–181356, Apr.2019.

[13] S. Colores, Sebastian, I. Aceves, R. Arreguin and J. Manuel. "Single image dehazing using a multilayer perceptron," *Journal of Electronic Imaging*, vol.27, no.4, pp:15–18, Apr.2018.

[14] D. Chen, M. He, Q. Fan, J. Liao, L. Zhang, D. Hou, L. Yuan, and G. Hua, "Gated Context Aggregation Network for Image Dehazing and Deraining," *IEEE Winter Conf. on Appl. of Comput. Vision* , pp:1375–1383, Apr.2019.

[15] X. Zheng, Y. Xiao and Y.Gong. "Research on remote sensing image dehazing method based on dark primary color prior, ". *Surveying and Spatial Geographic Information*, vol.43, no.1, pp: 57–60, Apr.2020.

[16] L.Xie, G.Xiong ,B.Yu, F.Zhu and B.Hu. "A new method for dehazing atmospheric degradation images based on dark channel priors," *Control Engineering*, vol.27, no.2, pp:207–211, Apr.2020.

[17] Z. Xu, S. Zhang, L. Guo, H. Huang, H. Wang and Q. Liu. "A method for defogging unmanned aerial vehicle remote sensing images,". *Communication Technology*, vol.53, no.10, pp:2442–2446, Apr.2020.

[18] S. Dhara, M. Roy, D. Sen, P. Biswas. "Color Cast Dependent Image Dehazing via Adaptive Airlight Refinement and Non-linear Color Balancing, ".*IEEE Transactions on Circuits and Systems for Video Technology,* vol.7, no.2, pp:12–14, Apr.2020.

[19] X. Cong, J. Zang and Q. Hu. "Image dehazing network based on dual learning," *Applied Optics.* vol.41, no.1, pp:94–99, Apr.2020.

[20] X. Cong, J. Zang and Q. Hu. "Anti fog network based on multi-scale dilated convolution,". *Applied Optics*. vol.41, no.6, pp:1207–1213, Apr.2020.

[21] C. He, C. Zhang, Q. Cheng, X. Jin and J. Yin, "A haze density aware adaptive perceptual single image haze removal algorithm," *IEEE International Conference on Information and Automation,* vol.10, no.1109, Apr.2016.

[22] G. Hou, J. Li, G. Wang, H. Yang, B. Huang and Z. Pan, "A novel dark channel prior guided variational framework for underwater image restoration," *Journal of Visual Communication and Image Representation*, Vol.66, no,102732, Apr.2020.

[23] H. Hui, Y. Yang, Y. Zhan, Y. Zhu and L. Zeng, "Bilateral Weighted Guided Filtering," vol.45, no.01, Apr.2024.